How to cite: *Angew. Chem. Int. Ed.* **2024**, e202412786
doi.org/10.1002/anie.202412786

Kinase Inhibitors

Thieno[3,2-*b*]pyridine: Attractive scaffold for highly selective inhibitors of underexplored protein kinases with variable binding mode

*Paula Martín Moyano, Tadeáš Kubina, Štěpán Owen Paruch, Aneta Jarošková, Jan Novotný, Veronika Skočková, Petra Ovesná, Tereza Suchánková, Polina Prokofeva, Bernhard Kuster, Michal Šmída, Apirat Chaikuad, Andreas Krämer, Stefan Knapp, Karel Souček, and Kamil Paruch**

Abstract: Protein kinases are key regulators of numerous biological processes and aberrant kinase activity can cause various diseases, particularly cancer. Herein, we report the identification of new series of highly selective kinase inhibitors based on the thieno[3,2-*b*]pyridine scaffold. The weak interaction of the thieno[3,2-*b*]pyridine core with the kinase hinge region allows for profoundly different binding modes all of which maintain high kinome-wide selectivity, as illustrated by the isomers **MU1464** and **MU1668**. Thus, this core structure provides a template of ATP-competitive but not ATP-mimetic inhibitors that are anchored at the kinase back pocket. Mapping the chemical space around the central thieno[3,2-*b*]pyridine pharmacophore afforded highly selective inhibitors of the kinase Haspin, exemplified by the compound **MU1920** that fulfils criteria for a quality chemical probe and is suitable for use in in vivo applications. However, despite the role of Haspin in mitosis, the inhibition of Haspin alone was not sufficient to elicit cytotoxic effect in cancer cells. The thieno[3,2-*b*]pyridine scaffold can be used in a broader context, as a basis of inhibitors targeting other underexplored protein kinases, such as CDKLs.

Introduction

The family of protein kinases contains more than 500 proteins that regulate numerous cellular signaling pathways in the cell.[1] Since aberrant activity of some protein kinases may lead to cancer, neurodegenerative, inflammatory, and autoimmune diseases,[2] targeting this class of enzymes represents one of the most dynamic areas of pharmaceutical research and a highly successful target class for drug development.[3]

Of more than 80 small-molecule kinase inhibitors approved for clinical use,[4] vast majority is represented by ATP-competitive inhibitors that are tightly anchored to the kinase hinge backbone. The ATP-binding site across the

[*] P. M. Moyano, T. Kubina, Š. O. Paruch, Prof. Dr. K. Paruch
Department of Chemistry, Faculty of Science,
Masaryk University
Kamenice 5, Brno 625 00 (Czech Republic)
E-mail: paruch@chemi.muni.cz

P. M. Moyano, Dr. K. Souček, Prof. Dr. K. Paruch
International Clinical Research Centre
St. Anne's University Hospital
Pekařská 53, Brno, 656 91 (Czech Republic)

A. Jarošková, J. Novotný, Dr. V. Skočková, Dr. T. Suchánková, Dr. K. Souček
Institute of Biophysics,
Czech Academy of Science
Královopolská 135, 612 00 Brno (Czech Republic)

A. Jarošková, J. Novotný, Dr. K. Souček
Department of Experimental Biology, Faculty of Science
Masaryk University
Kamenice 5, Brno 625 00 (Czech Republic)

Dr. P. Ovesná
Institute of Biostatistics and Analyses
Masaryk University
Kamenice 5, Brno 625 00 (Czech Republic)

Dr. P. Prokofeva, Prof. Dr. B. Kuster
Proteomics and Bioanalytics
Department of Molecular Life Sciences
School of Life Sciences
Technical University of Munich
Freising 85354 (Germany)

Dr. M. Šmída
CEITEC
Masaryk University
Kamenice 5, Brno 625 00 (Czech Republic)

Dr. A. Chaikuad, A. Krämer, Prof. Dr. S. Knapp
Institute for Pharmaceutical Chemistry, Structural Genomics Consortium
Johann Wolfgang Goethe-University
Max-von-Laue-Strasse 15, Frankfurt am Main, 60438 (Germany)

kinome is typically highly conserved, which makes identification of highly selective kinase inhibitors a non-trivial task.[5] Typical kinase inhibitor scaffolds are formed by nitrogen-containing heterocycles that enable interaction with the hinge region of a particular kinase.[6]

Proper choice of central scaffold can be crucial for achieving high selectivity against a kinase of choice.[7] We recently demonstrated that the weakly interacting furo[3,2-*b*]pyridine core can be used as the basis of highly selective kinase inhibitors of kinases CLK and HIPK.[8] Instead of forming strong hinge interactions, these inhibitors are anchored to the back pocket of the ATP site, which is narrow in some kinases such as Haspin, CLK and DYRK and DAPK family members, etc., because of an unusual large residue preceding the DFG motif (xDFG).[9]

In this work, we explored the applicability of the isosteric thieno[3,2-*b*]pyridine scaffold. The comparative ability of this motif to interact with the kinases hinge region was not obvious. On one hand, experimentally determined hydrogen bond basicity (pK_{BHX}) values of furan and thiophene are similar,[10] suggesting that interaction of thieno[3,2-*b*]pyridine would be analogous to furo[3,2-*b*]pyridine. On the other hand, hydrogen bonds dominated by electrostatic effects are stronger in O-containing systems vs. S-containing ones and calculated potential energy surfaces of hydrogen bonds involving sulfur are flat.[11]

While synthetic methodology for preparation of certain substituted thieno[3,2-*b*]pyridines is well documented in the literature,[12] reports on biologically active analogs are relatively scarce.[13] To our knowledge, there are only a handful of reports on thieno[3,2-*b*]pyridine-based kinase inhibitors. The broad-spectrum inhibitor of receptor tyrosine kinases sitravatinib,[14] is currently studied in clinical trials. Several reports describe substituted thieno[3,2-*b*]pyridines as inhibitors of c-Met/VEGF and src kinases.[15] Of note, none of them contains data on the inhibitors' selectivity profile nor the binding mode to the targeted kinases; and to our knowledge, there are no reports with a crystal structure of a thieno[3,2-*b*]pyridine derivative in a kinase.[16]

Results and Discussion

As a starting point, we prepared a sub-library of 3,5-disubstituted thieno[3,2-*b*]pyridines through a two-step sequence of chemoselective Suzuki couplings, utilizing commercially available 3-bromo-5-chlorothieno[3,2-*b*]pyridine (compound **A1** in Route A in Scheme 1 below). Of note, at that point there were no reports on the use of **A1** in the literature, despite the fact that the compound was commercially available. This first set of thieno[3,2-*b*]pyridine derivatives contained the compound **2**. Interestingly, this compound was found to have the kinome-wide selectivity

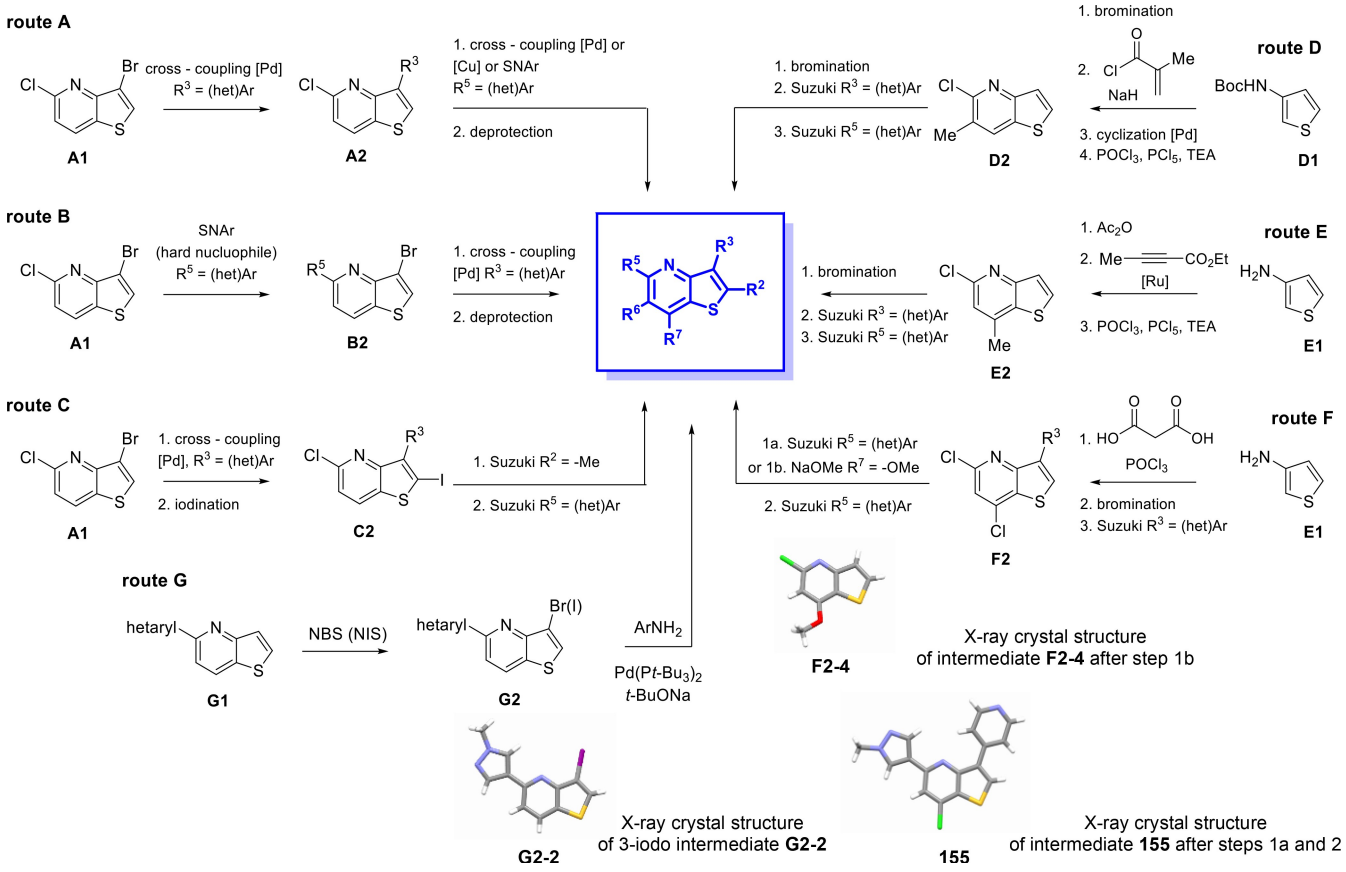

Scheme 1. Synthetic routes used for preparation of the target compounds.

profile quite comparable to that of the furo[3,2-*b*]pyridine **1** which we used as an early chemical starting point in our identification of potent and highly selective inhibitors of CLK kinases (Figure 1, Table S1).[8a] In complex with CLK1, the distance of the furo[3,2-*b*]pyridine oxygen to the hinge amide is too large (>4 Å) for an efficient polar interaction with the hinge. Instead, this inhibitor scaffold is anchored by polar interactions with the canonical VIAK back pocket salt bridge by the methyl pyrazole moiety.

Noteworthy was the activity of both compounds against the kinase Haspin (Haploid germ cell-specific nuclear protein kinase)—at 10 μM concentration we observed 97 % and 96 % inhibition, respectively (Table S1). Haspin, predominantly localized in the nucleus, is involved in the regulation of mitosis, where it specifically phosphorylates threonine 3 of histone H3 promoting centromeric recruitment of the chromosome passenger complex (CPC) during mitosis.[17] The kinase has been reported to be required for protection of cohesion at mitotic centromeres,[18] and inhibition of Haspin to impaire kinetochore recruitment of Bub1 and BubR1 kinases. Depletion of Haspin in human cells causes premature loss of centromeric cohesin from chromosomes in mitosis and failure of metaphase chromosome alignment, leading to activation of the spindle assembly checkpoint and mitotic arrest.[19]

Several previously identified Haspin inhibitors have been reported to possess anti-tumoral properties, suggesting that targeting Haspin could be applicable in oncology.[20] Unfortunately, these inhibitors display significant off-target activity.

We thus evaluated newly prepared compounds for activity against this kinase, along with selected off-targets of **2** listed in Table 1 below. The initial set of compounds contained also the analog **4** having excellent inhibitory activity for Haspin (IC_{50} = 89 nM). Pleasingly, the kinome-wide selectivity of this analog remained high and was clearly superior to that of the bioisosteric pyrazolo[1,5-*a*]pyrimidine **3** (Figure 2 and Table S2). Specifically, at 10 μM concentration, we observed >50 % inhibition of 32 kinases by the compound **4** vs. 156 kinases by the compound **3**.

We obtained X-ray crystal structures in complex with both compounds **3** and **4**, revealing significantly different binding modes (Figure 2).

Compound **3** interacted with Gly608 in the hinge region of the kinase through N1 of the pyrazolo[1,5-*a*]pyrimidine core, resulting in poor kinome wide selectivity. In contrast, the structure of Haspin with compound **4** showed that the methyl pyrazole substituent at position 5 of the thieno[3,2-*b*]pyridine scaffold formed a hydrogen bond with Gly608, positioning the thiophene moiety in proximity of the DYT motif in the kinase back pocket. Interestingly, the similarly active regiosomer **5** employed yet another binding mode, where the ligand was rotated approximately 90° relative to **4**. Here, the polar interaction with the hinge, again with Gly608 was established via the pyridine nitrogen atom, while still maintaining high selectivity across the kinome (Figure 2 and Table S2). In addition, the free nitrogen electron pair of the pyrazole moiety formed another hydrogen bond with the catalytic lysine (Lys511). The hinge interaction with Gly608 was the only common feature when comparing the different binding modes of these three very similar ligands. The different binding modes between **4** and **5** can be attributed to steric constraints related to the position of the methyl substituent. If **5** were to adopt the same binding mode as **4**, it would either collide with the hinge region or misalign the free electron pair of the pyrazole nitrogen, preventing it

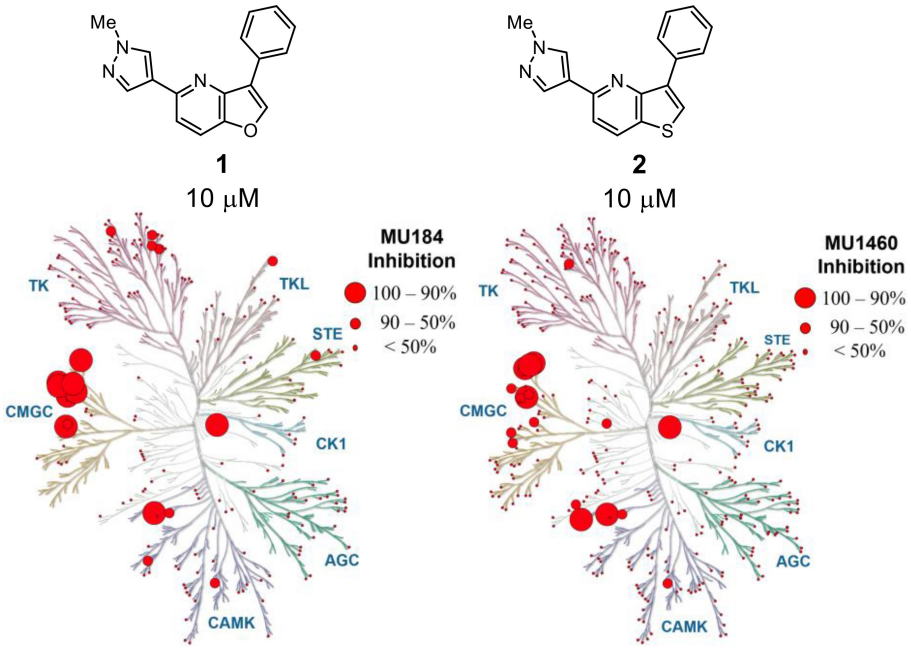

Figure 1. Comparison of the selectivity profiles of compounds **1** and **2**; tested at 10 μM concentration in a panel of 208 human kinases with ATP concentrations at Km (Eurofins).

Angewandte International Edition Chemie

Table 1: IC_{50} values (nM)[a] of selected compounds.[a] All compounds were tested in radiometric assays with ATP concentrations at Km (Eurofins). The complete data set for 153 target compounds is given in Table S4. N. d. = not determined.

Comp.	R^2	R^3	R^5	R^6	R^7	CDKL3	CDKL4	CLK2	DYRK2	Haspin	PIM1	TAF1L	TRB2
2 MU1460	H			H	H	280	280	4162	544	483	553	243	579
4 MU1464	H			H	H	198	343	>3000	656	89	309	228	883
5 MU1668	H			H	H	>3000	>3000	>3000	>3000	94	>3000	>3000	>3000
6	H			H	H	1319	2681	>3000	>3000	>3000	>3000	>3000	>3000
7	H			H	H	326	493	1117	568	18	98	217	672
8	H			H	H	409	706	872	>3000	49	1927	790	452
9 MU1920	H			H	H	>3000	>3000	>3000	>3000	6	>3000	2760	>3000
10	H			H	H	9285	8155	>3000	>3000	41	>3000	7685	9468
11	H			H	H	319	378	>3000	>3000	>3000	985	266	848
12	H			H	H	n.d.	n.d.	n.d.	n.d.	295	n.d.	n.d.	n.d.
13 MU2313	H			H	H	>3000	>3000	>3000	>3000	>3000	>3000	>3000	>3000
14	H			H	H	4574	5119	6891	>3000	1499	2958	4278	2947
15	H			H	H	86	78	2680	531	203	324	81	333
16	H			H	H	27	25	590	450	191	264	38	179

Comp.	R^2	R^3	R^5	R^6	R^7	CDKL3	CDKL4	CLK2	DYRK2	Haspin	PIM1	TAF1L	TRB2
17	H			H	H	17	36	430	287	57	298	9	17
18	H			H	H	43	36	806	157	23	134	33	85
19	H			H	H	>3000	>3000	>3000	>3000	39	>3000	>3000	>3000
20	H			H	H	53	105	189	413	5	45	50	80
21	H			H	H	>3000	>3000	>3000	>3000	23	>3000	>3000	>3000
22	Me			H	H	1739	1105	>3000	1006	1440	>3000	2013	2603
23	H			Me	H	1589	1982	>3000	>3000	1144	2808	1429	1391
24	H			Me	H	>3000	>3000	>3000	>3000	99	>3000	>3000	>3000
25	H			H	Me	2951	1621	>3000	>3000	2621	>3000	>3000	2279
26	H			H	Cl	2157	2382	>3000	>3000	253	>3000	1232	2563
27	H			H	OMe	937	916	>3000	>3000	427	>3000	649	1337
28	H			H	Cl	1725	1573	886	>3000	2	2139	1382	3883
29						>3000	>3000	>3000	>3000	>3000	>3000	>3000	>3000
30						938	976	>3000	>3000	99	>3000	1510	4792

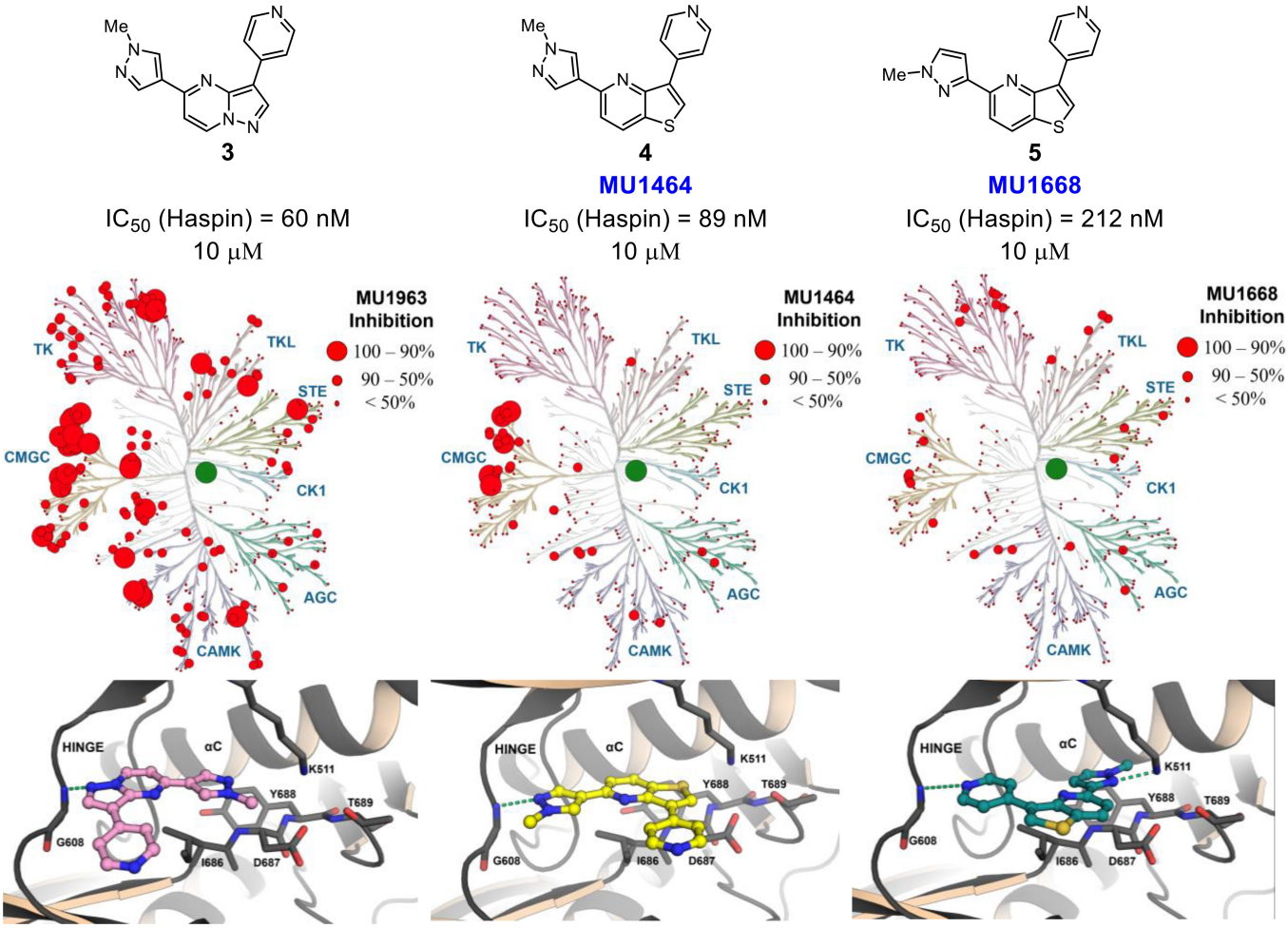

Figure 2. Comparison of **3**, **4**, and **5**. (top) Structures and Haspin IC_{50} values of the compounds **3**, **4**, and **5**. (middle) Selectivity profiles of the compounds **3**, **4**, and **5**; tested at 10 μM concentration in a panel of 413 human kinases with ATP concentrations at Km (Eurofins). Kinase Haspin is highlighted in green. (bottom) Binding modes of **3** (left), **4** (center), and **5** (right) in Haspin, determined by X-ray crystallography.

from forming a hydrogen bond with the hinge region. Conversely, if **4** were to adopt the binding mode of **5**, steric hindrance would occur in the back pocket, or the free electron pair of the pyrazole would not be positioned to act as a hydrogen bond acceptor for Lys511. The comparison between binding modes of compounds **3** and **4** was particularly intriguing. While it is relatively easy to see why **4** did not share the same binding mode as **3**—due to the inability of the thiophene sulfur to form a proper hydrogen bond with the hinge—the reverse scenario was less clear. In the absence of steric factors, we speculated that the pyrazolo[1,5-*a*]pyrimidine core served as a better hydrogen bond acceptor than the pyrazole alone, thus favoring this binding mode. This is consistent with observations that many kinase inhibitors and ATP interact with the hinge region via two conjugated ring systems.[21] The very different binding modes of the similar compounds **3** and **4** convincingly illustrated why **4** showed greater selectivity than **3**. While it is possible that **3** could adopt the binding mode of **4** with other kinases contributing to its promiscuity, this was not the case for **4**, which was restricted to only one possible binding mode. In summary, a combination of steric requirements in the back pocket and DYT region, together with the position and availability of hydrogen bond acceptors, dictated different binding modes, resulting in different selectivity profiles. Notably, we are not aware of any other cases where such minor structural changes resulted in so profoundly different binding modes.

The similar selectivity profiles and the almost exclusive selectivity of **5** for Haspin suggested that binding of both compounds is driven by back pocket interactions. Encouragingly, both **4** and **5** possessed significantly better kinome-wide selectivity than one of the state-of-the-art Haspin inhibitors—compound CHR6494[22] (Figure S1, Table S3). Our subsequent efforts were thus focused on further optimization of activity and selectivity for this kinase. In order to properly functionalize the thieno[3,2-*b*]pyridine core, we developed additional syntheses—routes B–G depicted in Scheme 1. All newly prepared compounds were profiled in radiometric kinase assays (Eurofins) against Haspin and seven selected off-target kinases listed in Table 1.

Routes A and B employing palladium-catalyzed couplings of the commercially available precursor **A1** with

boron-, nitrogen- and oxygen-based nucleophiles provided convenient modular access to a diverse set of 3,5-disubstituted thieno[3,2-*b*]pyridines. This methodology was further extended by route C that included additional iodination step, which allowed for flexible synthesis of 2,3,5-trisubstituted analogs (Scheme 1).

Through this protocol, we were able to identify optimal substituents at position 3 of the thieno[3,2-*b*]pyridine scaffold, namely, pyridine, pyrimidine and isothiazole—exemplified by the compounds **4**, **18** and **21** (Table 1).

Similarly, selected nitrogen-containing heterocycles were found to be optimal for functionalization of position 5 (cf. compounds **4**, **5** and **7** in Table 1).

Further selective improvement of the Haspin inhibitory activity was achieved through installation of the NH linker, as exemplified by compound **8** in Table 1. Additional substitution of the *N*-methylpyrazole substituent provided potent and selective Haspin inhibitor **9**. It should be noted that achieving high potency and selectivity required careful optimization of the substituent R^5—as illustrated by e.g. the structurally close analogs **11**, **13**, **14**, and the regioisomer **12**, which were dramatically less active (Table 1).

In order to explore the effect of substitution at the remaining positions of the thieno[3,2-*b*]pyridine core, we targeted the 6- and 7-methylated analogs of **4**.

Along this line, we developed the routes D and E that employ assembly of the pyridine ring through Pd-catalyzed Heck cyclization and Ru-catalyzed alkenylation, respectively (Scheme 1).[23] As illustrated by the compounds **23** and (in particular) **25**, these additional methylations had rather detrimental effect on the compounds' Haspin inhibitory activity (Table 1). Similarly, the 2-methylated analog **22**, prepared via route C, was also significantly less active (Table 1). We observed interesting chemoselectivity in the reactions with 5,7-dichlorinated thieno[3,2-*b*]pyridines **F2** in route F: while the nucleophilic substitution with sodium methoxide (step 1a) proceeded exclusively at position 7 (ultimately providing the analog **24**), palladium-catalyzed coupling (step 1b) afforded the 5-substituted intermediate that was elaborated into the target compound **26** (Scheme 1). We also found conditions for regioselective iodination of 5-substituted thieno[3,2-*b*]pyridines (route G in Scheme 1). This allowed for modular late-stage manipulation of position 3 and installation of 3-NH-linked substituents, exemplified by the compounds **15**, **16** and **17** with attractive inhibitory activity against the kinases CDKL3/4 and the bromodomain protein TAF1L (Table 1). Overall, by the routes A–G depicted in Scheme 1, we prepared and tested 153 new thieno[3,2-*b*]pyridine derivatives (Table S4).

Of the thieno[3,2-*b*]pyridine derivatives summarized in Tables 1 and S4, the compound **9** (**MU1920**) was found to possess optimal combination of high inhibitory potency against Haspin combined with significant selectivity against the off-target kinases CDKL3, CDKL4, CLK2, DYRK2, PIM1, TAF1L and TRB2 (Table 1). This high off-target selectivity of **9** compared favorably to the known nanomolar inhibitors of Haspin, namely CHR6494,[22] LDN192960, LDN209929,[24] 5-iodotubercidin (5-ITu),[25] SGI1776,[26] and CX6258.[27] As summarized in Table 2, all these Haspin

Table 2: IC_{50} values (nM)[a] of selected known Haspin inhibitors.[a] All compounds were tested in radiometric assays with ATP concentrations at Km (Eurofins).

Inhibitor		CDKL3	CDKL4	CLK2	DYRK2	Haspin	PIM1	TAF1L	TRB2	Inhibitor		CDKL3	CDKL4	CLK2	DYRK2	Haspin	PIM1	TAF1L	TRB2
5-ITu	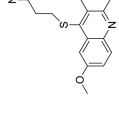	4	4	7	11	1	>3000	5	4	LDN 209929 ·2HCl		593	661	1544	87	172	174	395	67
HASPIN-IN-3	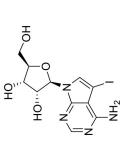	3	3	14	57	11	66	2	4	SGI 1776	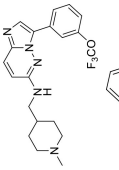	>3000	>3000	485	>3000	11	18	2504	2061
LDN 192960 ·HCl	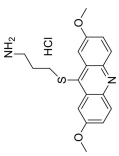	70	125	157	14	11	196	42	37	CX6258	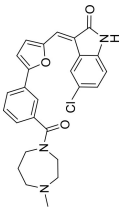	>3000	>3000	101	>3000	17	3	>3000	292

inhibitors were found to be less selective, underlining the potential of **9** to become a high-quality chemical biology probe. Thus, in order to further characterize **9**, we subjected it to kinome-wide profiling at 1 μM concentration in a panel of 413 human kinases (radiometric assay, Eurofins). To our delight, the compound showed exquisite selectivity and none of the kinases was inhibited more than 50 % (Figure 3A, Table S5).

The kinome-wide selectivity of **9** compared particularly favorably to that of the known Haspin inhibitor CHR6494 (Figure S1, Table S3). The crystal structure of **9** in Haspin (Figure 3A) revealed the binding mode analogous to that of **5**, and confirmed the compound as ATP-competitive inhibitor.

Next, we tested **9** for its ability to inhibit Haspin in the cell. In the HeLa and MDA-MB-231 cell lines, **9** elicited efficient inhibition of Haspin (with the IC_{50} values of 0.13 μM for HeLa and 0.35 μM for MDA-MB-231), indicated by the absence of phosphorylation of Thr3 in histone H3 (specific target of Haspin) as determined by western blot (Figure 3B and Figure S3). Cellular inhibition of Haspin with **9** was further confirmed by the ELISA assay in colon carcinoma cell line HT29, with the observed IC_{50} value of 94 nM (Figure 3D). However, up to 10 μM concentration, **9** did not elicit significant changes in the cell density (Figure 3E), viability (Figure 3F), and cycle distribution (Figure 3G) in HeLa and MDA-MB-231 cells. Also, similar concentrations of **9** did not affect the viability in large panel of 160 cancer cell lines ($EC_{50} > 50$ μM, Table S6) suggesting that selective inhibition of the kinase Haspin is not inherently cytotoxic. However, detailed analysis of cell cycle phase lengths by fluorescence time-lapse microscopy showed a significant increase in metaphase length in HeLa Fucci4 cells (Figure 3H).

The high cellular selectivity of **9** was confirmed in the Kinobeads assay[28] in human lysate generated from COLO-205, K-562, SK–N-BE(2), MV-4-11, and OVCAR-8 cells (described in the Supporting Information). Although Haspin was not bound by Kinobeads, our profiling revealed no other targets across 262 quantified kinases (Figure S4 and S5).

The less selective inhibitors **4** and **5** showed similar inhibitory activity against Haspin in HeLa and MDA-MB-231 cell lines (Figure S2). However, in contrast to **9**, these compounds at higher concentrations (10 μM) affected cell viability and induced changes in cell cycle (Figure S2), likely elicited by off-target inhibition.

In order to evaluate the potential of **9** to be used in vivo, we determined its pharmacokinetic parameters in mice. Pleasingly, the pharmacokinetic profile of **9** was good with the oral bioavailability 53 % at the 20 mpk dose. The compound administered orally at the 100 mpk dose was well tolerated (no signs of acute toxicity were observed in the animals), reaching plasma concentration > 0.75 μM for at least 10 hours (Figure 3I). The extent of plasma protein binding of **9** was found to be 91 % (mouse) and 95 % (human) (Figure 3J), the (kinetic) aqueous solubility 4 μM, and microsomal clearance (mouse) with CLint 149 μL/min/mg. Collectively, these pharmacological properties make the Haspin inhibitor **9** a suitable tool for in vivo studies.

The sub-series with NH-linked substituents at position 3 of the thieno[3,2-*b*]pyridine core was found to contain compounds with attractive inhibitory activity against CDKL kinases, exemplified by the compounds **15** and **16** (Table 1). This suggests that the thieno[3,2-*b*]pyridine scaffold can be used as the basis of efficient inhibitors of other underexplored kinases.

Conclusion

Identification of highly selective modulators of biological pathways ("chemical biology probes"), which can be used as key tools for elucidation of fundamental biological processes, represents one of the main challenges in the area of chemical biology research.[29] While in some cases sufficiently selective compounds have been identified (and frequently also served as starting points for development of novel drugs), for many other biological targets they still are to be discovered. Those include numerous underexplored protein kinases that are only emerging as potential targets for pharmacological inhibition.[3]

In this report, we identify the thieno[3,2-*b*]pyridine scaffold as an attractive platform for discovery of new highly selective kinase inhibitors. We demonstrate that the weakly interacting thieno[3,2-*b*]pyridine core allows for adoption of variable binding modes while keeping high kinome-wide selectivity, as illustrated by the isomers **4** (**MU1464**) and **5** (**MU1668**). This provides a rather unique opportunity for identification of chemical probes possessing high chemical similarity, but interacting orthogonally with the kinase of choice.

Of note, even though the thieno[3,2-*b*]pyridine core allows for adoption of variable binding modes (Figure 2), it does not act as an inert scaffold and contributes to overall inhibitory activity—as evidenced by the observation that the direct analog of **9** (**MU1920**) with geometrically similar central pharmacophore—i.e. the benzothiophene-based compound **30**—is significantly less potent (Table 1). Inactive were also thieno[3,2-*b*]pyridine sulfones, obtained by selective oxidation using hydrogen peroxide in the presence of trifluoroacetic acid—e.g. the compound **29**, obtained from the parent compound **4** (Table S4).

The exquisitely selective inhibitor of the kinase Haspin, compound **9** (**MU1920**), fulfills the criteria for a quality chemical biological probe and can be used for in vitro and in vivo studies, along with the negative control compound **13** (**MU2313**).

The data reported herein (Figure 3 and Table S6) strongly suggest that inhibition of Haspin alone is not sufficient to elicit anti-cancer effect, and that the antiproliferative activity of previously reported Haspin inhibitors is at least partly caused by inhibition of off-target kinases, e.g. PIM-1.[30] The results of complementary studies using shRNA-mediated knockdown of Haspin are rather ambiguous. While the Haspin depletion has been reported to cause loss of viability of certain cancer cells,[31] in other studies the

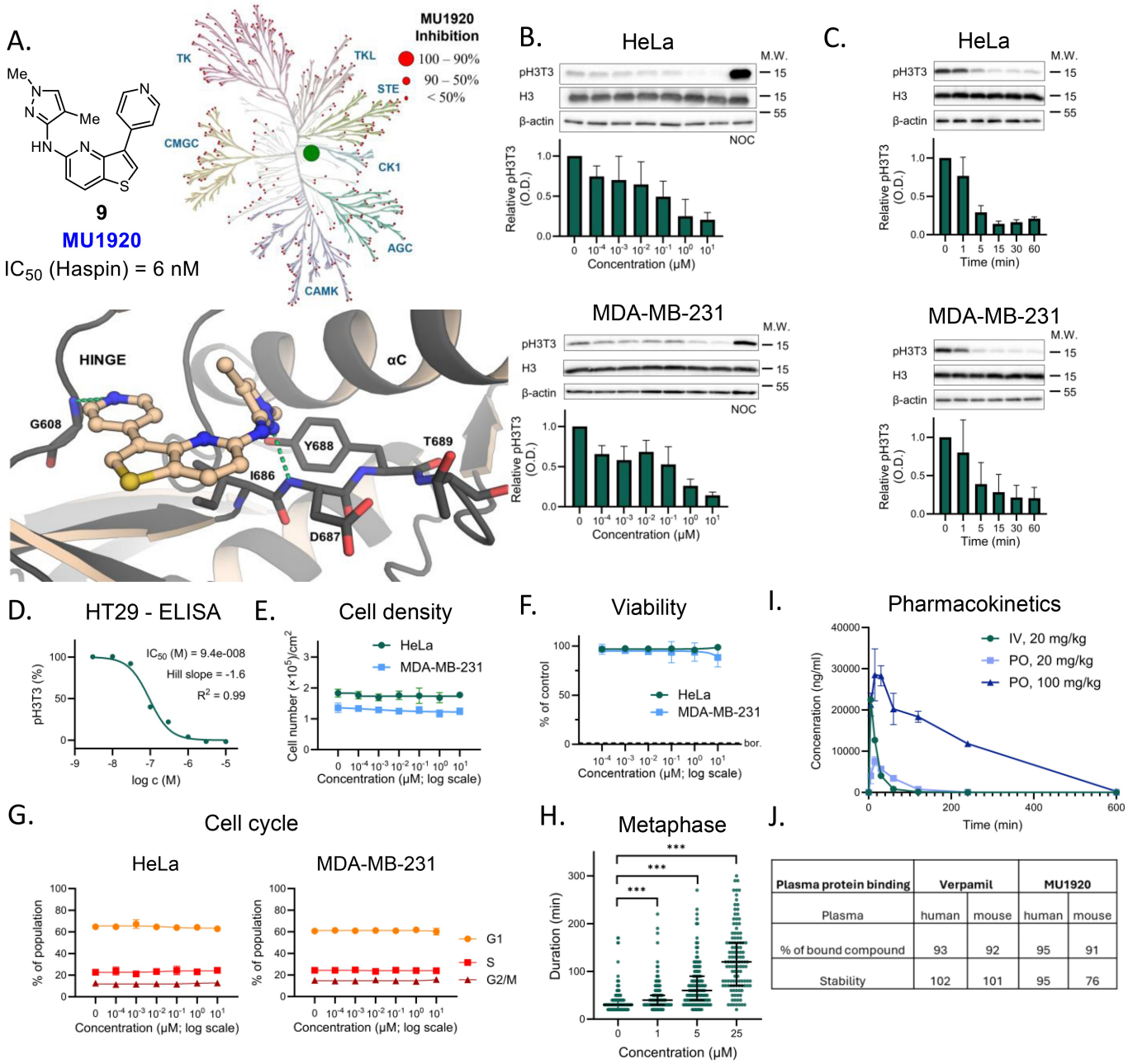

Plasma protein binding	Verpamil		MU1920	
Plasma	human	mouse	human	mouse
% of bound compound	93	92	95	91
Stability	102	101	95	76

Figure 3. Characterization of the Haspin inhibitor **9** (**MU1920**). **A.** Kinome-wide selectivity tested at 1 μM concentration in a panel of 413 human kinases with ATP concentrations at Km (Eurofins), X-ray crystal structure of **9** in Haspin. **B**. Inhibition of pH 3T3 in HeLa and MDA-MB-231 cells treated by series of concentrations of **9** (0.1 nM–10 μM) for 72 hours and analyzed by western blot. **C**. Inhibition of pH 3T3 in HeLa and MDA-MB-231 cells treated by 5 μM **9** for different time intervals (1–60 min) and analyzed by western blot. Nocodazole (NOC, 50 ng/ml) served as positive control. M.W. ~ molecular weight in kDa. O.D. ~ optical densitometry. Representative images for each condition were selected, quantification in bar plots represents mean ± SD ($n = 3$). **D.** In-cell ELISA assay measuring cellular inhibition of Haspin by **9** in colon carcinoma cell line HT29 (Reaction Biology). **E**. Number of HeLa and MDA-MB-231 cells treated by series of concentrations of **9** (0.1 nM–10 μM) for 72 hours. Cell growth was determined by counting of trypsinized cells using CASY TT system ($n = 3$, mean ± SD). **F**. Dose response curves of HeLa and MDA-MB-231 cells treated by series of concentrations of **9** (0.1 nM–10 μM) for 72 hours. 6 μM concentration of bortezomib (indicated by dashed line) was used as a positive control ($n = 3$, mean ± SD). Viability was determined by quantification of ATP with CellTiter-Glo One solution assay. Values were normalized to control (DMSO treated cells). **G.** Effect of 72-hour treatment with series of concentrations of **9** (0.1 nM–10 μM) on the distribution of cell cycle phases in HeLa and MDA-MB-231 cells. Cell cycle was measured by flow cytometry with propidium iodide staining ($n = 3$, mean ± SD). **H**. Metaphase duration of HeLa Fucci4 cells after treatment with series of concentrations of **9** (1, 5, 25 μM) by live-cell imaging microscopy within 24–48-hour window after treatment. Data shown is from 3 repetitions. Statistical evaluation was performed using generalized linear mixed model with biological repetitions as a random effect. *** indicates $p < 0.001$. **I**. IV and PO pharmacokinetic profile of **9** (dosed as water-soluble 2HCl salt) in the mouse at 20 mg/kg; PO PK profile of **9** at 100 mg/kg (Bienta). **J**. Plasma protein binding of **9** and Verapamil as reference (Bienta).

depletion was not accompanied by a significant impact on overall proliferation or viability.[32] It should be noted that generally, the phenotype obtained upon depletion may not always fully correspond to that elicited by small-molecule inhibition.[33] These include the scenarios when the protein of interest is part of a complex. This could also be the case for Haspin and its role in mitosis, mainly through the inhibition of Wapl occurring through direct physical interaction with Pds5 and phosphorylation of Wapl itself, as well as through the recruitment of the chromosome passenger complex, facilitated by Haspin's kinase activity and phosphorylation of Histone H3 at Thr3.[34] CRISPR/Cas9 knockout studies of Haspin have demonstrated that loss of expression leads to defective mitotic progression. However, this is not necessarily accompanied by a significant impact on overall proliferation or viability,[35] and the results of individual studies on the role of Haspin may be dependent on the particular experimental model, ability of tumor cells to adapt to perturbations in mitotic regulation, and the possibility that Haspin may have functions independent of its kinase activity.

Of note, recent reports suggest that selective Haspin inhibitors could be potentially useful for other therapeutic applications beyond oncology.[36]

The data summarized in Table 1 and Table S4 suggest that the thieno[3,2-*b*]pyridine scaffold can be utilized in a broader context, as the basis of inhibitors of other underexplored protein kinases, namely cyclin-dependent kinase-like kinases (CDKLs). CDKLs form a family of serine/threonine kinases whose biology still remains to be explored in greater detail;[37] nevertheless, the recently published studies suggest that their pharmacological inhibition can be attractive. CDKL2 has been recently recognized as a regulator of epithelial-mesenchymal transition of cancer cells.[38] The function of CDKL3 has not been fully elucidated; however, its inactivation has been shown to elicit inhibition of proliferation, migration, and cell cycle progression of human cholangiocarcinoma cells.[39] Conversely, high levels of CDKL3 promote progression of osteosarcoma and negatively correlate with the patient survival.[40] High levels of CDKL4 have been found in malignant bone tumor (chordomas),[41] while its silencing improved the sensitivity of colorectal carcinoma cells to the treatment with oxaliplatin.[42] In mouse models, genetic or pharmacological CDKL5 inhibition has been shown to mitigate nephrotoxic and ischemia-associated acute kidney injury.[43] The neuroactive steroid ganaxolone was recently approved in EU for the treatment of seizures in people with CDKL5 deficiency disorder.[44] However, very few CDKL inhibitors have been reported, with CDKLs rather being their off-targets,[37,39] with unknown selectivity. The compounds CAF-181 and SNS-032 posted on the Structural Genomics Consortium web site[45] suffer from insufficient potency or selectivity, respectively. To our knowledge, the only CDKL inhibitors with acceptable potency and selectivity are the CDKL5 inhibitors B1, B4, and B12, reported in 2023.[46]

Acknowledgements

The Paruch group gratefully acknowledges the support provided by the following sources of funding: European Structural and Investment Funds, Operational Programme Research, Development and Education—„Preclinical Progression of New Organic Compounds with Targeted Biological Activity" (Preclinprogress)—CZ.02.1.01/0.0/0.0/16_025/0007381, the project CZ-OPENSCREEN: National Infrastructure for Chemical Biology (CZ-OPENSCREEN LM2023052), Ministry of Health of the Czech Republic—Agency for Healthcare Research of the Czech Republic (grant number NW24-08-00280), and Bader Philanthropies. This work was also supported by the EC through the Horizon Europe project IMPULSE (grant agreement number 101132028), by the Czech Science Foundation (grant no. 23–06472S, KS), and by the project National Institute for Cancer Research (Programme EXCELES, ID Project no. LX22NPO5102)—Funded by the European Union—Next Generation EU (KS, AJ). The authors would like to thank Iva Lišková, Martina Urbánková and Kateřina Svobodová for technical assistance. SK is grateful for support by the Structural Genomics Consortium (SGC), a registered charity (no: 1097737) that receives funds from Bayer AG, Boehringer Ingelheim, Bristol Myers Squibb, Genentech, Genome Canada, EU/EFPIA/OICR/McGill/KTH/Diamond, Innovative Medicines Initiative 2 Joint Undertaking [EUbOPEN grant 875510], Janssen, Pfizer and Takeda. SK is also supported by the German Cancer Research Center DKTK, the Frankfurt Cancer Institute (FCI) and the German cancer aid (Krebshilfe) project TACTIC. Open Access publishing facilitated by Masarykova univerzita, as part of the Wiley - CzechELib agreement.

Conflicts Of Interest

The authors declare no conflict of interest.

Data Availability Statement

The data that support the findings of this study are available in the supplementary material of this article.

Keywords: Haspin · thieno[3,2-*b*]pyridine · chemical probe · kinase inhibitor · selectivity

[1] P. Cohen, D. Cross, P. A. Jänne, *Nat. Rev. Drug Discovery* **2021**, *20*, 551–569.
[2] F. M. Ferguson, N. S. Gray, *Nat. Rev. Drug Discovery* **2018**, *17*, 353–377.
[3] M. M. Attwood, D. Fabro, A. V. Sokolov, S. Knapp, H. B. Schiöth, *Nat. Rev. Drug Discovery* **2021**, *20*, 839–861.
[4] R. Roskoski, *Pharmacol. Res.* **2024**, *200*, 107059.
[5] a) M. E. Breen, M. B. Soellner, *ACS Chem. Biol.* **2015**, *10*, 175–189; b) K. Umezawa, I. Kii, *Molecules* **2021**, *26*, 651.
[6] V. Sharma, M. Gupta, *Chem. Biol. Drug Des.* **2022**, *100*, 968–980.

[7] a) J. J.-L. Liao, *J. Med. Chem.* **2007**, *50*, 409–424; b) M. W. Karaman, S. Herrgard, D. K. Treiber, P. Gallant, C. E. Atteridge, B. T. Campbell, K. W. Chan, P. Ciceri, M. I. Davis, P. T. Edeen, R. Faraoni, M. Floyd, J. P. Hunt, D. J. Lockhart, Z. V. Milanov, M. J. Morrison, G. Pallares, H. K. Patel, S. Pritchard, L. M. Wodicka, P. P. Zarrinkar, *Nat. Biotechnol.* **2008**, *26*, 127–132.

[8] a) V. Němec, M. Hylsová, L. Maier, J. Flegel, S. Sievers, S. Ziegler, M. Schröder, B. T. Berger, A. Chaikuad, B. Valčíková, S. Uldrijan, S. Drápela, K. Souček, H. Waldmann, S. Knapp, K. Paruch, *Angew. Chem. Int. Ed.* **2019**, *58*, 1062–1066; b) V. Němec, L. Maier, B. T. Berger, A. Chaikuad, S. Drápela, K. Souček, S. Knapp, K. Paruch, *Eur. J. Med. Chem.* **2021**, *215*, 113299.

[9] M. Schröder, A. N. Bullock, O. Fedorov, F. Bracher, A. Chaikuad, S. Knapp, *J. Med. Chem.* **2020**, *63*, 10224–10234.

[10] C. Laurence, K. A. Brameld, J. Graton, J.-Y. Le Questel, E. Renault, *J. Med. Chem.* **2009**, *52*, 4073–4086.

[11] F. Wennmohs, V. Staemmler, M. Schindler, *J. Chem. Phys.* **2003**, *119*, 3208–3218.

[12] D. S. Black, J. Cossy, C. V. Stevens, *Comprehensive Heterocyclic Chemistry IV. A Review of the Literature 2008–2021.* Elsevier, Amsterdam, The Netherlands, **2022**, Volume 10. Chapter 6, 135–183.

[13] a) R. M. V. Abreu, I. C. F. R. Ferreira, R. C. Calhelha, R. T. Lima, M. H. Vasconcelos, F. Adega, R. Chaves, M. R. P. Queiroz, *Eur. J. Med. Chem.* **2011**, *46*, 5800–5806; b) M. R. P. Queiroz, D. Peixoto, R. C. Calhelha, P. Soares, T. dos Santos, R. T. Lima, J. F. Campos, R. M. V. Abreu, I. C. F. R. Ferreira, M. H. Vasconcelos, *Eur. J. Med. Chem.* **2013**, *69*, 855–862.

[14] P. P. Patwardhan, K. S. Ivy, E. Musi, E. de Stanchina, G. K. Schwartz, *Oncotarget* **2016**, *7*, 4093–4109.

[15] a) O. Saavedra, S. Claridge, L. Zhan, F. Raeppel, M. Granger, S. Raeppel, M. Mannion, F. Gaudette, N. Zhou, L. Isakovic, N. Bernstein, R. Déziel, H. Nguyen, N. Beaulieu, C. Beaulieu, I. Dupont, J. Wang, A. R. Macleod, J. M. Besterman, A. Vaisburg, *Bioorg. Med. Chem. Lett.* **2009**, *19*, 6836–6839; b) D. H. Boschelli, B. Wu, A. C. B. Sosa, H. Durutlic, J. J. Chen, Y. Wang, J. M. Golas, J. Lucas, F. Boschelli, *J. Med. Chem.* **2005**, *48*, 3891–3902; c) M. R. P. Queiroz, R. C. Calhelha, L. A. Vale-Silva, E. Pinto, M. S. J. Nascimento, *Eur. J. Med. Chem.* **2010**, *45*, 5732–5738; d) S. Claridge, F. Raeppel, M. Granger, N. Bernstein, O. Saavedra, L. Zhan, D. Llewellyn, A. Wahhab, R. Deziel, J. Rahil, N. Beaulieu, H. Nguyen, I. Dupont, A. Barsalou, C. Beaulieu, I. Chute, S. Gravel, M. Robert, S. Lefebvre, M. Dubay, R. Pascal, J. Gillespie, Z. Jin, J. Wang, J. M. Besterman, A. R. MacLeod, A. Vaisburg, *Bioorg. Med. Chem. Lett.* **2008**, *18*, 2793–2798.

[16] Checked through ligand search in KLIFS database https://klifs.net/search.php.

[17] J. Dai, S. Sultan, S. S. Taylor, J. M. G. Higgins, *Genes Dev.* **2005**, *19*, 472–488.

[18] A. De Antoni, S. Maffini, S. Knapp, A. Musacchio, S. Santaguida, *J. Cell Biol.* **2012**, *199*, 269–284.

[19] J. M. G. Higgins, *Chromosoma* **2010**, *119*, 137–147.

[20] N. G. Amoussou, A. Bigot, C. Roussakis, J.-M. H. Robert, *Drug Discovery Today* **2018**, *23*, 409–415.

[21] S. Röhm, A. Krämer, S. Knapp, *Function, Structure and Topology of Protein Kinases. In: Laufer, S. (eds) Proteinkinase Inhibitors. Topics in Medicinal Chemistry*, Springer, Cham, **2022**, Volume 36.

[22] D. Huertas, M. Soler, J. Moreto, A. Villanueva, A. Martinez, A. Vidal, M. Charlton, D. Moffat, S. Patel, J. McDermott, J. Owen, D. Brotherton, D. Krige, S. Cuthill, M. Esteller, *Oncogene* **2012**, *31*, 1408–1418.

[23] a) Q. F. Hu, T. T. Gao, Y. J. Shi, Q. Lei, L. T. Yu, *RSC Adv.* **2018**, *8*, 13879–13890; b) R. Manikandan, M. Jeganmohan, *Org. Lett.* **2014**, *16*, 652–655.

[24] G. D. Cuny, M. Robin, N. P. Ulyanova, D. Patnaik, V. Pique, G. Casano, J. F. Liu, X. Lin, J. Xian, M. A. Glicksman, R. L. Stein, J. M. G. Higgins, *Bioorg. Med. Chem. Lett.* **2010**, *20*, 3491–3494.

[25] a) D. Massillon, W. Stalmans, G. van de Werve, M. Bollen, *Biochem. J.* **1994**, *299*, 123–128; b) A. De Antoni, S. Maffini, S. Knapp, A. Musacchio, S. Santaguida, *J. Cell Biol.* **2012**, *199*, 269–284.

[26] a) L. S. Chen, W. G. Wierda, S. Redkar, D. J. Bearss, V. Gandhi, *Blood* **2008**, *112*, 4199; b) S. M. Mumenthaler, P. Y. B. Ng, A. Hodge, D. Bearss, G. Berk, S. Kanekal, S. Redkar, P. Taverna, D. B. Agus, A. Jain, *Mol. Cancer Ther.* **2009**, *8*, 2882–2893.

[27] M. Haddach, J. Michaux, M. K. Schwaebe, F. Pierre, S. E. O'Brien, C. Borsan, J. Tran, N. Raffaele, S. Ravula, D. Drygin, A. Siddiqui-Jain, L. Darjania, R. Stansfield, C. Proffitt, D. Macalino, N. Streiner, J. Bliesath, M. Omori, J. P. Whitten, K. Anderes, W. G. Rice, D. M. Ryckman, *ACS Med. Chem. Lett.* **2012**, *3*, 135–139.

[28] M. Reinecke, B. Ruprecht, S. Poser, S. Wiechmann, M. Wilhelm, S. Heinzlmeir, B. Kuster, G. Médard, *ACS Chem. Biol.* **2019**, *14*, 655–664.

[29] M. M. Mader, J. Rudolph, I. V. Hartung, D. Uehling, P. Workman, W. Zuercher, *Cancer Dis.* **2023**, *13*, 1–16.

[30] a) A. L. Merkel, E. Meggers, E. Ocker, *Expert Opin. Invest. Drugs* **2012**, *21*, 425–436; b) D. Drygin, M. Haddach, F. Pierre, D. M. Ryckman, *J. Med. Chem.* **2012**, *55*, 8199–8208; c) L. Chen, W. Mao, C. Ren, J. Li, J. Zhang, *J. Med. Chem.* **2024**, *67*, 38–64.

[31] X. Han, T. Kuang, Y. Ren, Z. Lu, Q. Liao, W. Chen, *Exp. Cell Res.* **2019**, *385*, 111605.

[32] T. N. Cartwright, R. J. Harris, S. K. Meyer, A. M. Mon, N. A. Watson, C. Tan, A. Marcelot, F. Wang, S. Zinn-Justin, P. Traktman, J. M. G. Higgins, *Sci. Rep.* **2022**, *12*, 11210.

[33] a) W. Weiss, S. Taylor, K. M. Shokat, *Nat. Chem. Biol.* **2007**, *3*, 739–744; b) Z. A. Knight, K. M. Shokat, *Cell* **2007**, *128*, 425–430.

[34] R. Quadri, S. Sertic, M. Muzi-Falconi, *Cell. Signal.* **2022**, *93*, 110303.

[35] L. Zhou, C. Liang, Q. Chen, Z. Zhang, B. Zhang, H. Yan, F. Qi, M. Zhang, Q. Yi, Y. Guan, X. Xiang, X. Zhang, S. Ye, F. Wang, *Curr. Biol.* **2017**, *27*, 992–1004.

[36] a) H. Tanaka, H. Matsushita, K. Tokuhiro, A. Fukunari, Y. Ando, *Biology* **2023**, *12*, 320; b) L. M. Rodrigo, D. R. Nyholt, *Genes* **2021**, *12*, 689; c) R. Quadri, S. Sertic, A. Ghilardi, D. Rondelli, G. R. Gallo, L. Del Giacco, M. Muzi-Falconi, *Int. J. Mol. Sci.* **2021**, *22*, 7753.

[37] P. Canning, K. Park, J. Goncalves, C. Li, C. J. Howard, T. D. Sharpe, L. J. Holt, L. Pelletier, A. N. Bullock, M. R. Leroux, *Cell Rep.* **2018**, *22*, 885–894.

[38] Q. Shao, F. Wang, Y. Xu, X. Zhang, W. Tang, Y. Feng, Y. Li, *BioMed Res. Int.* **2020**, article 1712723.

[39] J. Zhang, G. Su, Z. Tang, L. Wang, W. Fu, S. Zhao, Y. Ba, B. Bai, P. Yue, Y. Lin, Z. Bai, J. Hu, W. Meng, L. Qiao, X. Li, X. Xie, *Front. Plant Physiol.* **2018**, *9*, article 234.

[40] A. He, L. Ma, Y. Huang, H. Zhang, W. Duan, Z. Li, T. Fei, J. Yuan, H. Wu, L. Liu, Y. Bai, W. Dai, Y. Wang, H. Li, Y. Sun, Y. Wang, C. Wang, T. Yuan, Q. Yang, S. Tian, M. Dong, R. Sheng, D. Xiang, *Life Sci. Alliance* **2020**, *3*, e202000648.

[41] R. L. Walker, F. J. Hornicek, Z. Duan, *Biochim. Biophys. Acta Rev. Cancer* **2022**, *1877*, 188812.

[42] M. Lin, Y. Zhang, A. Li, E. Tang, J. Peng, W. Tang, Y. Zhang, L. Lu, Y. Xiao, Q. Wei, L. Yin, H. Li, *Oncotarget* **2015**, *6*, 16774–16785.

[43] J. Y. Kim, Y. Bai, L. A. Jayne, R. D. Hector, A. K. Persaud, S. S. Ong, S. Rojesh, R. Raj, M. J. H. H. Feng, S. Chung, R. E. Cianciolo, J. W. Christman, M. J. Campbell, D. S. Gardner, S. D. Baker, A. Sparreboom, R. Govindarajan, H. Singh, T. Chen, M. Poi, K. Susztak, S. R. Cobb, N. S. Pabla, *Nat. Commun.* **2020**, *11*, article 1924.
[44] Y. N. Lamb, *Drugs* **2022**, *82*, 933–940.
[45] https://openlabnotebooks.org/selective-cdkl2-inhibitors-molecular-modeling/.
[46] a) A. Castano, M. Silvestre, C. I. Wells, J. L. Sanderson, C. A. Ferrer, H. W. Ong, Y. Lang, W. Richardson, J. A. Silvaroli, F. M. Bashore, J. L. Smith, I. M. Genereux, K. Dempster, D. H. Drewry, N. S. Pabla, A. N. Bullock, T. A. Benke, S. K. Ultanir, A. D. Axtman, *eLife* **2023**, *12*, e88206; b) H. W. Ong, Y. Liang, W. Richardson, E. R. Lowry, C. I. Wells, X. Chen, M. Silvestre, K. Dempster, J. A. Silvaroli, J. L. Smith, H. Wichterle, N. S. Pabla, S. K. Ultanir, A. N. Bullock, D. H. Drewry, A. D. Axtman, *ACS Chem. Neurosci.* **2023**, *14*, 1672–1685.

Manuscript received: July 8, 2024
Accepted manuscript online: November 6, 2024
Version of record online: ■■, ■■

Research Article

Kinase Inhibitors

P. M. Moyano, T. Kubina, Š. O. Paruch, A. Jarošková, J. Novotný, V. Skočková, P. Ovesná, T. Suchánková, P. Prokofeva, B. Kuster, M. Šmída, A. Chaikuad, A. Krämer, S. Knapp, K. Souček, K. Paruch* **e202412786**

Thieno[3,2-*b*]pyridine: Attractive scaffold for highly selective inhibitors of underexplored protein kinases with variable binding mode

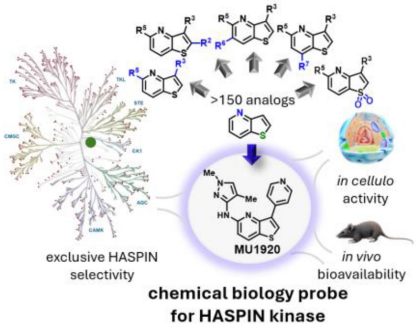

Weak interaction of thieno[3,2-*b*]pyridine with the kinase hinge region allows for design of highly selective inhibitors of underexplored kinases with variable binding modes. The newly identified chemical biology probe **MU1920** targets the kinase Haspin with exquisite kinome-wide selectivity. Our observations suggest that the thieno[3,2-*b*]pyridine scaffold can be used also for identification of inhibitors of other "non-routine" protein kinases, e.g. CDKLs.